NOISE REDUCTION FOR PATH TRACED IMAGING OF PARTICIPATING MEDIA

Qing Xu[1,2]*, Yu Liu*[1]*, Ruijie Zhang*[1]*, Shiqiang Bao*[1]*, Riccardo Scopigno*[2]*, and Mateu Sbert*[3]

[1] School of Computer Science and Technology, Tianjin University
Weijin Road 92, 300072, Tianjin, China
phone: +86 22 27406538, fax: +86 22 27406538, email: qingxu@tju.edu.cn
[2] Networking Lab, Istituto Superiore Mario Boella
Via P.C. Boggio 61, 10138, Torino, Italy
phone: +39 011 2276603, fax: +39 011 2276299, email: scopigno@ismb.it
[3] Graphics and Imaging Laboratory, Universitat de Girona
Edifici P4, Campus Montilivi, 17071, Girona, Spain
phone: +34 972 418419, fax: +34 972 418792, email: mateu@ima.udg.edu

ABSTRACT

The paper proposes a new noise reduction technique counteracting noise in path traced images: a filter kernel, referred to as *gradient kernel*, is defined exploiting the gradient direction of particle density of participating media. The gradient kernel is combined with the bilateral filter, so to enhance it: the rationale is to perform Monte Carlo noise suppression while preserving details in path traced images, exploiting the information inherent in the 3D scenes. The proposed method is applied to path traced images, the rendering results of multiple and non-isotropic light scattering in non-homogeneous participating media. The experimental results show that the novel approach behaves remarkably well both quantitatively and qualitatively.

1. INTRODUCTION

A participating medium is composed of a lot of particles. When the light travels in the medium and interacts with the particles, the initial light distribution experiences angular, spatial and temporal spread, causing a complex radiance distribution. Monte Carlo based global illumination (MCGI) algorithms is one of the most important methods for realistic imaging of multiple and anisotropic light scattering in inhomogeneous participating media and can give the physically correct solutions to the light transport problem [1]. MCGI usually employs path tracing [2]: unfortunately path traced images suffer from the well known Monte Carlo noise, in particular when a low sampling rate is used.

Filtering is a good and straightforward way to remove noise, so it is typically carried out also as a post-processing stage to remove Monte Carlo noise, by making use of some classic filters. McCool [3] exploited the anisotropic diffusion approach with the aid of depth and normal information. Xu and Pattanaik [4] extended the bilateral filter [5], by operating Gaussian kernel for each pixel and then applying the standard bilateral filters. In this paper, a new way to improve the bilateral filter is proposed, aimed at reducing Monte Carlo noise in path traced images for 3D scenes — especially with inhomogeneous participating media. Upon exploiting the gradient direction of particle density of participating media, a function (named gradient kernel function) is introduced and incorporated into the bilateral filter to help remove noise: its main potential comes from that it is complementary to the range kernel adopted in bilateral filter.

The remainder of the paper is organized as follows. In section 2, the novel filter is described; results are demonstrated in section 3; finally conclusions are presented.

2. THE PROPOSED FILTER

2.1 Monte Carlo Noise in Path Traced Images

Because each pixel value is obtained stochastically and independently by Monte Carlo sampling and Monte Carlo integration, noise always exists in the path traced imagings. Basically Monte Carlo noise appearing in path traced images presents as the mixture of inter-pixel incoherence and outliers [4] and, even worse, heavy noise may group to form large noise patches — see Figs. 2(b) and 3(b) as examples. So, on the one hand, Monte Carlo noise behaves as inter-pixel incoherence — the pixels in a smooth neighborhood seem to fluctuate and vary irregularly, and this could be counteracted by locally averaging pixel values, being somewhat similar to the classic Gaussian noise. On the other hand, Monte Carlo noise presents as outliers, pixels noticeably dissimilar to their neighbors.

Since bilateral filter is based on locally averaging pixel values, it can smooth additive Gaussian noise well [5] but, reversely, it is not effective against outliers or impulse noise [6]. Garnett et al. [6] improved the bilateral filter for the mixed Gaussian and impulsive noise.

2.2 Rationale of the Proposed Filter

Despite bilateral filter effectively reduces noise, it can not completely remove it — as shown in the examples Figs. 2(c) and 3(c). This is due at least to two concurrent factors: the intrinsic definition of bilateral filtering and the stochastic nature of Monte Carlo imaging. In fact bilateral filtering carries out denoising process pixel by pixel, considering the neighborhood of each pixel, evaluating both spatial and radiometric similarity — the latter is fundamental to preserving edges. Unfortunately the stochastic Monte Carlo process can make two neighboring pixels, within the same smooth image region, largely different. As a result the bilateral filter may keep some noise intact. The proposed goal is to benefit from the deterministic 3D information drawn from the inhomogeneous participating media to improve the bilateral filter by making it context-aware.

Thanks to NSFC by China (60879003), Polo ICT of Regione Piemonte (MOMA project-Proposal 8024-7133), MEC by Spain (TIN2010-21089-C03-01) and Generalitat de Catalunya (2009-SGR-643) for funding.

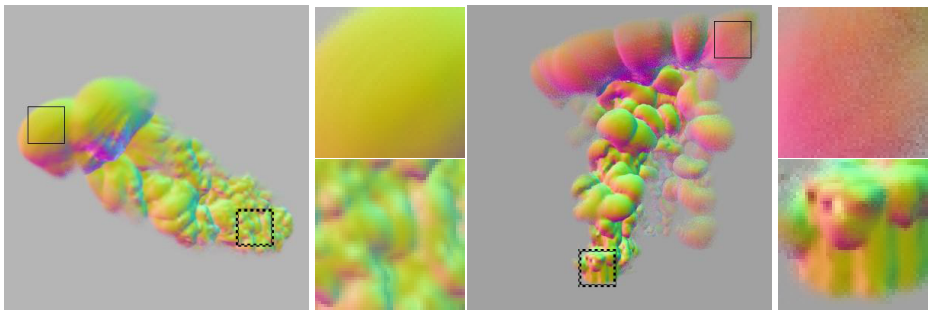

(a) Cloud (b) Smoke

Figure 1: Visualization of pixel gradient direction

From here on "surface" is called the boundary between the participating media and the others in a 3D scene: a 3D surface can be smooth or frequently fluctuating — as shown in the areas within the windows with continuous and dotted lines in Figs. 2(a) and 3(a). Since the non-homogeneous participating media include particles in spatially varying density, the gradient direction of particle density is proposed as a direct indicator of surface contours of participating media. In essence, close locations have similar gradient directions in a smooth surface area, and *vice versa*. Fig. 1 displays the visualization of the pixel gradient directions (a detailed explanation is provided in Section 2.3): different colors correspond to different gradient directions to vividly depict the surface contours of participating media – smooth areas do not present many colors, while areas with high variations illustrate a lot of them — see Figs. 2(a) and 3(a).

Intuitively the radiometric differences among neighboring pixels are positively correlated with the differences among 3D neighbors on the surface of the participating media, so the vectorial differences ("the distances") between the gradient directions of particle density correspond to the contour differences and can be utilized to establish the "gradient kernel". The gradient kernel can complement the range kernel and enhance the classic bilateral filter.

2.3 Gradient Kernel and Filtering

The participating media in a 3D scene are described by 3D volumetric uniform grids with varying density of particles: each grid includes a description of the gradient direction of particle density in its center. Path gradient direction is gathered during path tracing for each sample path, as the gradient direction of particle density at the intersection of the path with the surface of the participating media. More precisely gradient direction is computed as a 3D spatial linear interpolation of the gradient directions of particle density at the surrounding grids.

Given the gradient direction of a sample path, the gradient direction of a pixel is defined as the average on the gradients of the paths contributing to such pixel.

If G_X and G_Y are the normalized gradient directions respectively at the image pixels X and Y, and θ_{XY} is the intersection angle of G_X and G_Y, the gradient kernel is defined in the following way:

$$w_G = e^{-\frac{(1-\cos\theta_{XY})^2}{2\sigma_G^2}}, \qquad (1)$$

where σ_G is the typical Gaussian parameter acting on the shape and regulating the weight of the kernel itself. Qualitatively, w_G is high when θ_{XY} is small, and *vice versa*, due to the cosine function; θ_{XY}, the angular difference between G_X and G_Y, varies in the range $[0^o, 180^o]$. So w_G is a weighting function designed on the "distance" between the pixel gradient directions, and it is, by construction, complementary to the radiometric difference between the pixels.

Let L_X be the pixel value at a pixel X, and R_X be the set of pixels in a $(2n+1)\times(2n+1)$ neighborhood of X. w_G is integrated into the bilateral filtering (normally the bilateral filter can be defined as $\hat{L}_X = \frac{\sum_{Y\in R_X} w_D w_L L_Y}{\sum_{Y\in R_X} w_D w_L}$ [5]) to produce the new filter:

$$\hat{L}_X = \frac{\sum_{Y\in R_X} w_D(w_L + w_G)L_Y}{\sum_{Y\in R_X} w_D(w_L + w_G)}, \qquad (2)$$

where $\hat{L}_X$ is the restored value of X, L_Y is the pixel value of Y in R_X, and w_D and w_L are the standard domain kernel $w_D = e^{-\frac{|X-Y|^2}{2\sigma_D^2}}$ and range kernel $w_L = e^{-\frac{|L_X-L_Y|^2}{2\sigma_L^2}}$ (σ_D and σ_L are the Gaussian parameters). The gradient kernel is directly added to the range kernel because it is functionally compatible and, due to its complementary definition, it is expected to improve noise suppression capability.

3. IMPLEMENTATION AND RESULTS

In this section a comparative analysis is carried out between the proposed solution and 3 filtering approaches relevant to the application: bilateral filter [5] (Bilateral), extended bilateral filter [4] (Ext-bilateral) and trilateral filter [6] (Trilateral). Just as in the usual Monte Carlo denoising [4], 4 filters postprocess the indirect illumination component of the path traced images. Considering that the new filter is specific for participating media, only the pixels showing participating media are respectively processed by 4 filters; the other ones are handled only by the bilateral filter. All the filters use a window size of 13×13 and are run in the CIE-Lab color space, as suggested in [4] and [5] respectively.

The optimal settings for the new filter have been experimentally determined: σ_D, σ_L and σ_G are 2, 10 and 3 respectively; more in general, σ_D in $[2,3]$ and σ_L in $[10,20]$ work well, almost in the same way. For each of the filter compared, the parameters have been tested exhaustively to obtain the best possible result — σ_d=2, σ_r=20 for the bilateral filter; σ_d=3, σ_r=10 for the extended bilateral filter; σ_S=2 (1st pass)

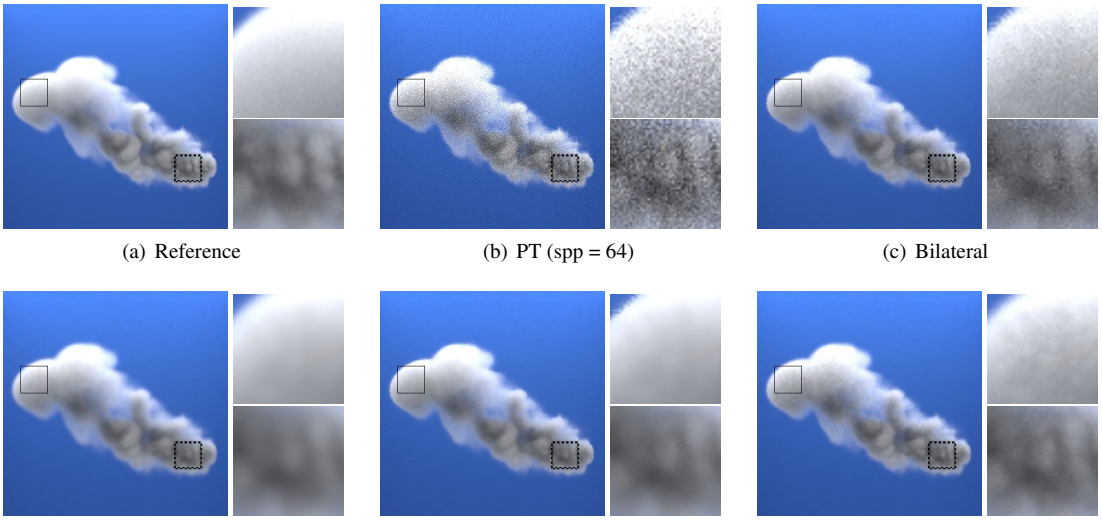

(a) Reference (b) PT (spp = 64) (c) Bilateral

(d) Ext-bilateral (e) Trilateral (f) Proposed filtering

Figure 2: Filtered results for Cloud (SPP=64)

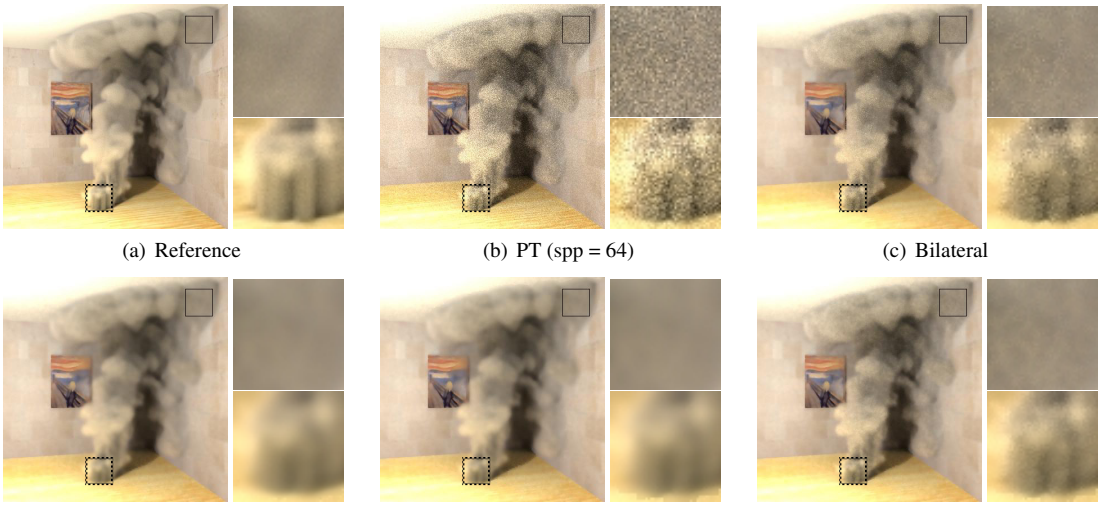

(a) Reference (b) PT (spp = 64) (c) Bilateral

(d) Ext-bilateral (e) Trilateral (f) Proposed filtering

Figure 3: Filtered results for Smoke (SPP=64)

and 2.236 (2nd pass), σ_I=40, σ_J=50 for the trilateral filter. As a matter of fact, the optimum filtering parameters used in this paper depend upon the amounts of noise and image texture contained in the images, and also upon the surface contours of participating media: their systematic investigation is an open topic (though some published studies have attempted to automatically define the parameters used in the bilateral filter, see [7] as an example) and will be left for our future work.

Two sets of test images of size 400×400 pixels are based on two test scenes, Cloud and Smoke, which specifically include non-homogeneous participating media. The reference images of the two test scenes by path tracing with 2000 samples per pixel (spp=2000) are used as the "gold" standard (ground truth) to quantify the errors of the filtered images, and the error metric is Root Mean Square (RMS)

$$RMS = \sqrt{\frac{\sum_{i=1}^{n}((L_i - L_i^{ref})^2 + (a_i - a_i^{ref})^2 + (b_i - b_i^{ref})^2)}{n}}, \quad (3)$$

Table 1: Comparison of filtered results in RMS and runtime

		Cloud		Smoke	
SPP	Method	RMS	Runtime (s)	RMS	Runtime (s)
spp=16	PT	8.62	-	8.15	-
	Bilateral	2.09	65	2.23	64
	Ext-bilateral	1.78	73	2.14	76
	Trilateral	1.56	438	2.12	477
	Proposed	1.67	76	2.06	78
spp=36	PT	5.79	-	5.57	-
	Bilateral	1.86	62	1.859	62
	Ext-bilateral	1.54	72	1.82	75
	Trilateral	1.21	443	1.82	479
	Proposed	1.34	75	1.67	78
spp=64	PT	4.33	-	4.23	-
	Bilateral	1.66	63	1.74	62
	Ext-bilateral	1.33	72	1.66	76
	Trilateral	1.08	444	1.62	487
	Proposed	1.21	75	1.47	79

where (L_i, a_i, b_i) and $(L_i^{ref}, a_i^{ref}, b_i^{ref})$ are the i-th pixel values

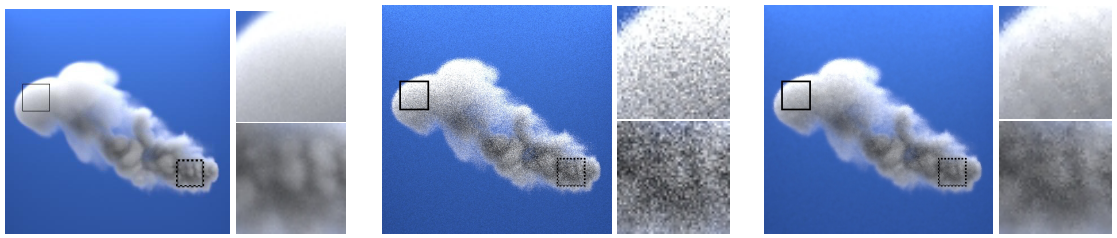

(a) Reference (b) PT (spp = 36) (c) Bilateral

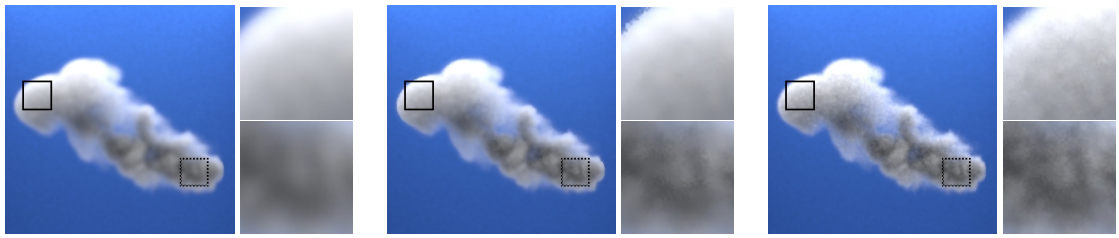

(d) Ext-bilateral (e) Trilateral (f) Proposed filtering

Figure 4: Filtered results for Cloud (SPP=36)

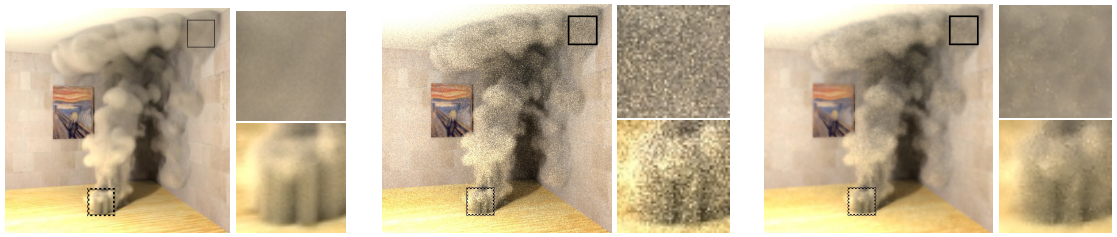

(a) Reference (b) PT (spp = 36) (c) Bilateral

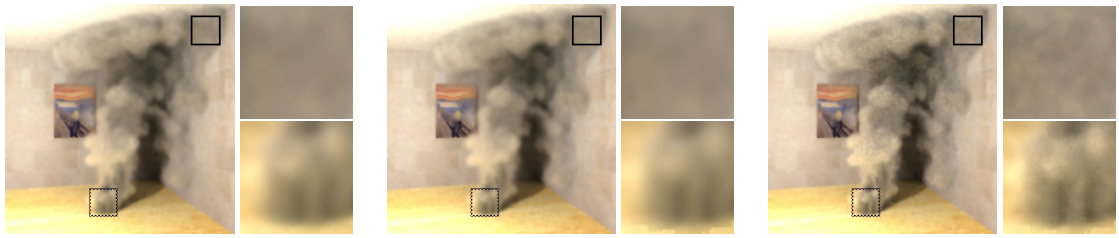

(d) Ext-bilateral (e) Trilateral (f) Proposed filtering

Figure 5: Filtered results for Smoke (SPP=36)

of the filtered image and of the reference image, defined in the CIE-Lab color space.

The path traced (PT) images and the filtered images are shown in Figs. 2-7. It is clear how the bilateral filter leaves some evident noise untouched, while the proposed filter contemporaneously improves noise reduction and edge preservation. Compared with the extended bilateral filter and the trilateral filter, the proposed one preserves image details largely better while noise suppression performance is almost the same.

The 4 filters for the path traced images have been tested at different noise levels (the images are produced with different *spp*): the RMS and runtime results (runtime is obtained from our test-bed software in C++ on a Windows PC with Intel Pentium E2180 2.00GHz CPU and 2GB RAM) are listed in Table 1. The RMS results by the proposed technique are mostly better than those by the others, with several exceptions in which data by the proposed method are a little worse than those by the trilateral filter — but, notably, in these cases the restored images by the trilateral filter are seriously blurred and involve an excessive runtime. The runtime by the new method is satisfactory — it is less than one-sixth of that by the trilateral filter, and is only a little worse than that by the extended bilateral filter.

All in all, the quantitative and qualitative results, and also the running time achieved by the proposed method are favorable, though, some comparable, when compared with those by the competitive algorithms.

4. CONCLUSIONS

This paper has presented a new filter aimed at counteracting Monte Carlo noise in path traced imaging of inhomogeneous participating media. The proposed contribution comes from the use of the gradient direction of particle density of participating media as a condition improving the bilateral filter.

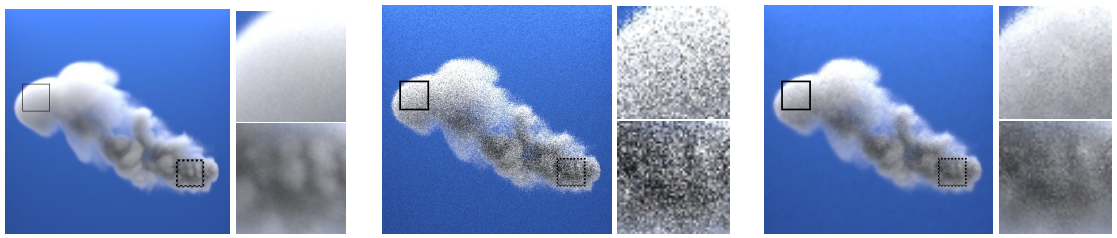

(a) Reference (b) PT (spp = 16) (c) Bilateral

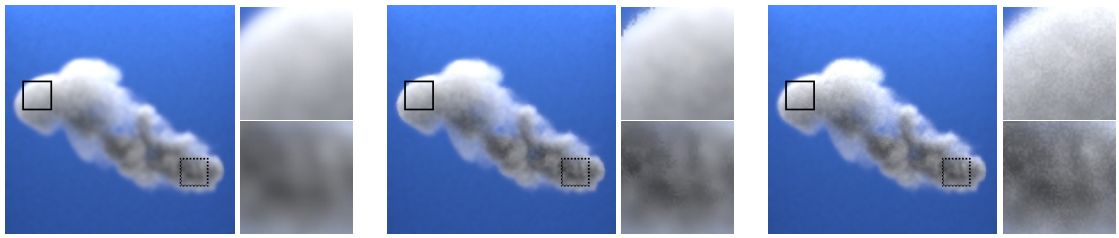

(d) Ext-bilateral (e) Trilateral (f) Proposed filtering

Figure 6: Filtered results for Cloud (SPP=16)

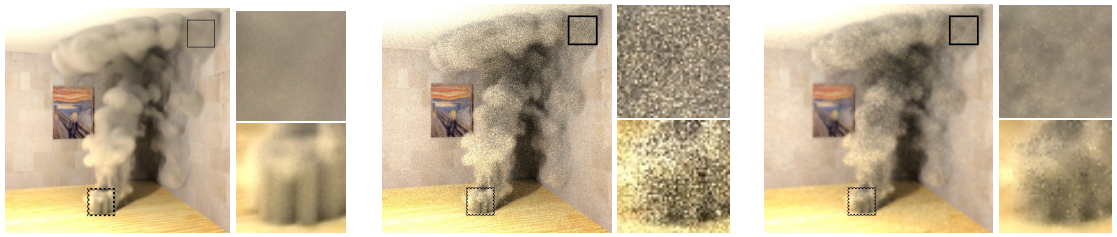

(a) Reference (b) PT (spp = 16) (c) Bilateral

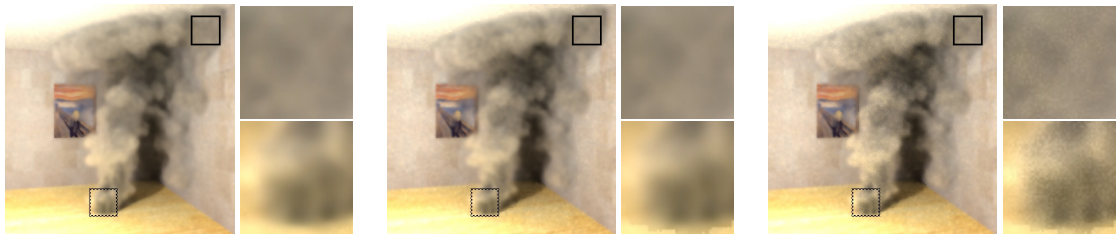

(d) Ext-bilateral (e) Trilateral (f) Proposed filtering

Figure 7: Filtered results for Smoke (SPP=16)

Experimental results confirm the improved performance of noise reduction and edge preservation achieved by the novel technique.

The proposed technique can be speeded up, for example, by using modern hardware such as (Graphics Processing Unit, GPU): this constitutes our future work.

REFERENCES

[1] A. Keller, T. Kollig, M. Sbert, and L. Szirmay-Kalos, "Efficient Monte Carlo and Quasi-Monte Carlo rendering techniques," *Eurographics 2003 Tutorial*, 2003.

[2] T. Kajiya, "The rendering equation," *Computer Graphics*, vol. 20, Aug. 1986.

[3] M. D. McCool, "Anisotropic diffusion for Monte Carlo noise reduction," *ACM Transactions on Graphics*, vol. 18, pp. 171–194, Apr. 1999.

[4] R-F. Xu and S. N. Pattanaik, " A novel Monte Carlo noise reduction operator," *IEEE Computer Graphics and Applications*, vol. 25, pp. 31–35, Mar.-Apr. 2005.

[5] C. Tomasi and R. Manduchi, "Bilateral filtering for gray and color images," in *Proc. Sixth International Conference on Computer Vision (ICCV)*, Bombay, India, January 4-7. 1998, pp. 839–846.

[6] R. Garnett, T. Huegerich, C. Chui, and W-J. He, "A universal noise removal algorithm with an impulse detector," *IEEE Transactions on Image Processing*, vol. 14, pp. 1747–1754, Nov. 2005.

[7] C. Liu, R. Szeliski, S-B. Kang, C.L. Zitnick, and W.T. Freeman, "Automatic Estimation and Removal of Noise from a Single Image," *IEEE Transactions on Pattern Analysis and Machine Intelligence*, vol. 30, pp. 299–314, Feb. 2008.